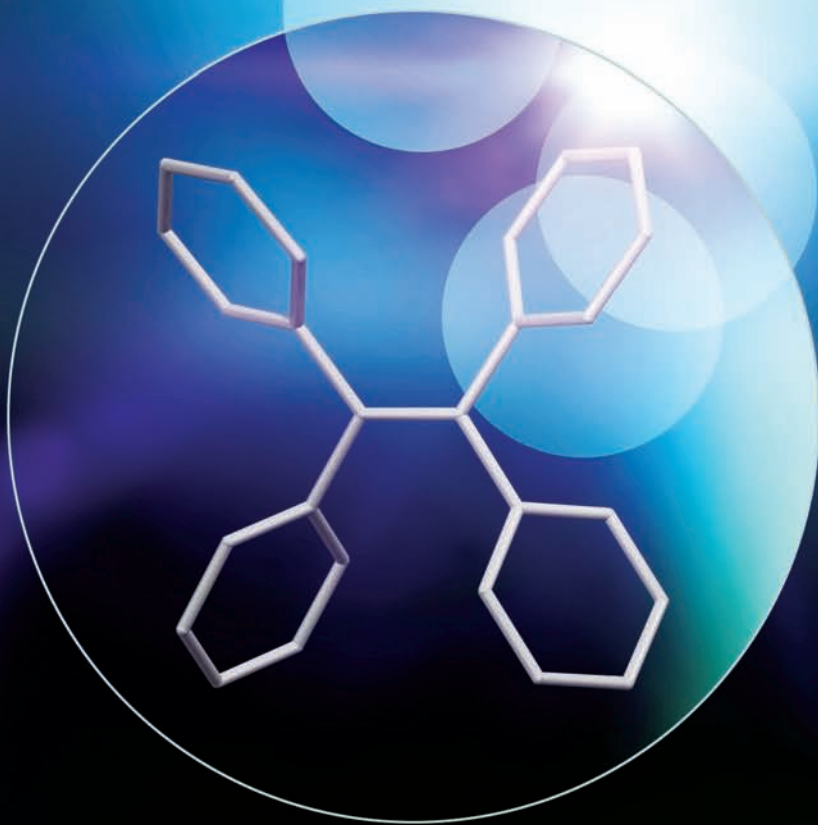


EDITORS ANJUN QIN AND BEN ZHONG TANG

AGGREGATION-INDUCED EMISSION

FUNDAMENTALS



WILEY

Aggregation-Induced Emission: Fundamentals

Aggregation-Induced Emission: Fundamentals

Edited by

ANJUN QIN

Department of Polymer Science and Engineering, Zhejiang University, China

AND

BEN ZHONG TANG

Department of Chemistry, The Hong Kong University of Science and Technology, China

WILEY

This edition first published 2014
© 2014 John Wiley & Sons, Ltd

Registered office
John Wiley & Sons Ltd, The Atrium, Southern Gate, Chichester, West Sussex, PO19 8SQ, United Kingdom

For details of our global editorial offices, for customer services and for information about how to apply for permission to reuse the copyright material in this book please see our website at www.wiley.com.

The right of the author to be identified as the author of this work has been asserted in accordance with the Copyright, Designs and Patents Act 1988.

All rights reserved. No part of this publication may be reproduced, stored in a retrieval system, or transmitted, in any form or by any means, electronic, mechanical, photocopying, recording or otherwise, except as permitted by the UK Copyright, Designs and Patents Act 1988, without the prior permission of the publisher.

Wiley also publishes its books in a variety of electronic formats. Some content that appears in print may not be available in electronic books.

Designations used by companies to distinguish their products are often claimed as trademarks. All brand names and product names used in this book are trade names, service marks, trademarks or registered trademarks of their respective owners. The publisher is not associated with any product or vendor mentioned in this book.

Limit of Liability/Disclaimer of Warranty: While the publisher and author have used their best efforts in preparing this book, they make no representations or warranties with respect to the accuracy or completeness of the contents of this book and specifically disclaim any implied warranties of merchantability or fitness for a particular purpose. It is sold on the understanding that the publisher is not engaged in rendering professional services and neither the publisher nor the author shall be liable for damages arising herefrom. If professional advice or other expert assistance is required, the services of a competent professional should be sought.

The advice and strategies contained herein may not be suitable for every situation. In view of ongoing research, equipment modifications, changes in governmental regulations, and the constant flow of information relating to the use of experimental reagents, equipment, and devices, the reader is urged to review and evaluate the information provided in the package insert or instructions for each chemical, piece of equipment, reagent, or device for, among other things, any changes in the instructions or indication of usage and for added warnings and precautions. The fact that an organization or Website is referred to in this work as a citation and/or a potential source of further information does not mean that the author or the publisher endorses the information the organization or Website may provide or recommendations it may make. Further, readers should be aware that Internet Websites listed in this work may have changed or disappeared between when this work was written and when it is read. No warranty may be created or extended by any promotional statements for this work. Neither the publisher nor the author shall be liable for any damages arising herefrom.

Library of Congress Cataloging-in-Publication Data

Aggregation-induced emission : fundamentals / edited by Professor Ben Zhong

Tang and Dr Anjun Qin.

pages cm

Includes bibliographical references and index.

ISBN 978-1-118-39430-4 (cloth)

1. Electroluminescent devices. 2. Photoemission. 3. Aggregation (Chemistry) 4. Organosilicon compounds—Optical properties. I. Tang, Ben Zhong. II. Qin, Anjun.

TK7871.68.A44 2014

620.1'1295—dc23

2013016216

A catalogue record for this book is available from the British Library.

Print ISBN: 9781118394304

Set in 10/12pt Times by Thomson Digital, Noida, India.

Contents

<i>List of Contributors</i>	<i>xiii</i>
<i>Preface</i>	<i>xvii</i>
1 Synthesis of Siloles (and Germoles) that Exhibit the AIE Effect	1
<i>Joyce Y. Corey</i>	
1.1 Introduction	1
1.2 Background	2
1.3 Synthesis of Siloles	4
1.3.1 Reductive dimerization of tolan	4
1.3.2 Intramolecular cyclization of dialkynylsilanes	7
1.3.3 Intramolecular cyclization of dialkynylsilanes utilizing borane reagents	10
1.3.4 Synthesis of siloles using transition metal reagents	12
1.4 Modification of Preformed Siloles	14
1.4.1 Reactions at silicon centers	14
1.4.2 Reactions of a ring carbon center	15
1.5 Related Germole Methodology	15
1.5.1 Germoles produced by metathesis and exchange reactions	15
1.5.2 Germoles from other methods	16
1.5.3 Photoluminescence and AIE of germoles	18
1.6 Metallaindenes and Metallafluorenes of Si and Ge	19
1.6.1 Methods for the formation of silaindenes and germaindenes	19
1.6.2 Methods for the formation of metallafluorenes	21
1.7 Oligomers and Polymers of Metalloles and Benzene-Annulated Metalloles	25
1.7.1 Oligomers that contain silole units connected at the 1,1- and 2,5-positions	25
1.7.2 Polysiloles and silole polymers connected through 2,5-positions	26
1.7.3 Polymers with silole pendants and hyperbranched polymers	27
1.7.4 Polybenzosiloles and ladder polymers	28
1.7.5 Polymers that contain silafluorenes	29
1.7.6 Germoles in oligomers and polymers	30
1.8 Summary and Future Directions	31
References	33

2	Aggregation-Induced Emission in Group 14 Metalloles (Siloles, Germales, and Stannoles): Spectroscopic Considerations, Substituent Effects, and Applications	39
	<i>Jerome L. Mullin and Henry J. Tracy</i>	
2.1	Introduction	39
2.1.1	The group 14 metalloles	41
2.2	Characteristics of AIE in the Group 14 Metalloles	44
2.2.1	Aryl-substituted siloles	44
2.2.2	Aryl-substituted germales and stannoles	47
2.3	Origins of AIE in Group 14 Metalloles: Restricted Intramolecular Rotation	48
2.3.1	Effect of solvent viscosity	48
2.3.2	Effect of temperature	48
2.3.3	Room-temperature glasses	49
2.3.4	Effect of pressure	49
2.3.5	Excited-state lifetimes	49
2.3.6	Molecular geometry	50
2.3.7	Aggregate nanoparticle morphology	50
2.3.8	Internal structural control of intramolecular rotations	50
2.4	Polymer Films and Polymerized Siloles	51
2.5	Applications of AIE-Active Metalloles	53
2.5.1	Electrooptical devices	53
2.5.2	Chemical sensors	53
	References	54
3	Aggregation-Induced Emission of 9,10-Distyrylanthracene Derivatives and Their Applications	61
	<i>Bin Xu, Jibo Zhang and Wenjing Tian</i>	
3.1	Introduction	61
3.2	AIE Molecules Based on 9,10-Distyrylanthracene	63
3.2.1	Small molecules	63
3.2.2	Macromolecules	64
3.3	AIE Mechanism of 9,10-Distyrylanthracene Molecule Systems	65
3.4	Application of AIE Luminogens Based on 9,10-Distyrylanthracene	67
3.4.1	Solid-state emitters	67
3.4.2	Piezochromism	72
3.4.3	Fluorescent sensors and probes	74
3.4.4	Bioimaging	75
3.5	Conclusion	80
	Acknowledgments	80
	References	80
4	Diaminobenzene-Cored Fluorophores Exhibiting Highly Efficient Solid-State Luminescence	83
	<i>Masaki Shimizu</i>	
4.1	Introduction	83
4.2	1,4-Bis(alkenyl)-2,5-dipiperidinobenzenes	86
4.3	1,4-Diamino-2,5-bis(arylethenyl)benzenes	89
4.4	2,5-Diaminoterephthalates	93

4.5	2,5-Bis(diarylamino)-1,4-diaroylbenzenes	95
4.6	Applications	99
4.7	Conclusion	102
	Acknowledgments	102
	References	103
5	Aggregation-Induced Emission in Organic Ion Pairs	105
	<i>Suzanne Fery-Forgues</i>	
5.1	Introduction	105
5.2	Historical Background	106
5.3	Preparation and Control of the Fluorophore Arrangement	107
5.3.1	Type of interactions	107
5.3.2	Preparation	107
5.3.3	Influence of the nature of the counterion on the fluorophore arrangement	108
5.3.4	Influence of stoichiometry on the AIE effect	111
5.4	AIE-Active Organic Ion Pairs in Nano- and Microparticles	111
5.4.1	Controlled preparation of nanoparticles	112
5.4.2	Nanoparticles for biomedical imaging	114
5.4.3	Preparation of nanocrystals, nanofibers, and reticulated materials	114
5.5	Applications as Fluorescent Probes and Sensors for Analytical Purposes	115
5.5.1	Detection of small electrolytes	115
5.5.2	Detection of polyelectrolytes	116
5.6	Perspectives	122
	Acknowledgments	122
	References	123
6	Aggregation-Induced Emission Materials: the Art of Conjugation and Rotation	127
	<i>Jing Huang, Qianqian Li and Zhen Li</i>	
6.1	Introduction	127
6.2	Rotation and Conjugation in AIE Molecules	128
6.3	Design of Functional Materials by Tuning the Conjugation Effect and Restricting Rotations	134
6.3.1	Some AIE molecules with blue emission through modification of the conjugation between the construction blocks	135
6.3.2	Some sensing systems by selectively controlling rotation	142
6.3.3	Some other systems utilizing the AIE concept	145
6.4	Outlook	151
	References	152
7	Red-Emitting AIE Materials	155
	<i>Xiao Yuan Shen, Anjun Qin and Jing Zhi Sun</i>	
7.1	Introduction	155
7.2	Basic Principles of Molecular Design for Red-Emitting Materials	156
7.3	Acquirement of Red-Emitting AIE Materials by Reconstruction of Traditional Red-Emitting Molecules	158
7.4	Preparation of Red-Emitting Materials by Introduction of Electron Donors/Acceptors into AIE-Active Molecules	162

7.5	Outlook	164
	Acknowledgments	165
	References	165
8	Properties of Triarylamine Derivatives with AIE and Large Two-Photon Absorbing Cross-Sections	169
	<i>Jianli Hua, He Tian and Hao Zhang</i>	
8.1	Introduction	169
8.2	Design and Synthesis of Triarylamine Derivatives with AIE and 2PA	170
8.3	AIE Properties of Triarylamine Derivatives	170
8.3.1	AIE properties of diketopyrrolopyrrole (DPP)-based triarylamine derivatives	170
8.3.2	AIE properties of starburst triarylamine derivatives based on cyano-substituted diphenylaminestrylbenzene	173
8.3.3	AIE properties of multibranched triarylamine end-capped triazines	174
8.4	One-Photon and Two-Photon Absorption Properties of Triarylamine Derivatives with AIE	176
8.5	Application of Triarylamine Materials with AIE and 2PA	180
8.5.1	Fluorescence switching	180
8.5.2	Organic light-emitting diodes	180
8.5.3	Fluorescence probes for Hg^{2+}	180
8.6	Conclusion	181
	References	182
9	Photoisomerization and Light-Driven Fluorescence Enhancement of Azobenzene Derivatives	185
	<i>Mina Han and Yasuo Norikane</i>	
9.1	Introduction	185
9.2	Photoisomerization and Fluorescence of Azobenzene Derivatives	186
9.2.1	Ground-state structure of azobenzene	186
9.2.2	Reversible isomerization of azobenzene	187
9.2.3	Sterically hindered azobenzene derivatives	188
9.2.4	Fluorescence from azobenzene derivatives	190
9.3	Aggregation-Induced Emission (AIE)	191
9.4	Fluorescence from Azobenzene-Based Aggregates	193
9.4.1	Light-driven self-assembly and fluorescence enhancement	194
9.4.2	Factors affecting fluorescence enhancement of azobenzenes	195
9.4.3	Modulation of fluorescence color	196
9.4.4	Fluorescent organic films	198
9.5	Conclusion	199
	References	199
10	Supramolecular Structure and Aggregation-Induced Emission	205
	<i>Hongyu Zhang and Yue Wang</i>	
10.1	Introduction	205
10.2	Hydrogen Bonding-Based Molecular Dimer and AIE	206
10.2.1	The role of hydrogen bonds in AIE	206
10.2.2	AIE and single crystal structures	208

10.2.3	Relationship between supramolecular structures and AIE	209
10.2.4	Amplified spontaneous emission (ASE) property	210
10.3	Quinacridine Derivatives with 1D Aggregation-Induced Red Emission	210
10.3.1	Contradiction between 1D self-assembly and AIE	210
10.3.2	Design of novel QA with AIE and 1D self-assembly	211
10.3.3	AIE behavior	212
10.3.4	Morphology transition from 0D nanostructures to 1D microwires	214
10.3.5	1D self-assembly	214
10.3.6	Crystal structure	215
10.4	Multi-Stimuli-Responsive Fluorescence Switching of AIE/AIEE Luminogens	217
10.4.1	Mechanism of stimuli-responsive fluorescence switching	217
10.4.2	Design strategy towards stimuli-responsive AIE/AIEE molecules	218
10.4.3	AIE phenomenon in neutral and acid states	218
10.4.4	Molecular and supramolecular structures in crystal	220
10.4.5	Multi-stimuli-responsive AIE switching	220
10.4.6	Multi-stimuli-responsive fluorescence of other AIE/AIEE molecules	221
10.5	Pt···Pt Interaction-Induced Emissive and Conductive 1D Crystals	222
10.5.1	AIE of organometallic complexes	222
10.5.2	Pt···Pt interaction-induced luminescent crystals	223
10.5.3	1D nano-/micro aggregation and photophysical properties	223
10.5.4	Vapor-responsive emission behavior of nanowires	225
10.5.5	Pt···Pt interaction-induced 1D semiconductor	225
10.6	Conclusion	226
	References	227
11	Aggregation-Induced Emission in Supramolecular π-Organogels	233
	<i>Pengchong Xue and Ran Lu</i>	
11.1	Introduction	233
11.2	Organogels Based on Discotic Molecules with AIE	234
11.2.1	Triphenylbenzene-cored discotic molecules	234
11.2.2	Other discotic gelators	237
11.3	Organogels Based on Rod-Like Molecules with AIE	238
11.3.1	Styrene derivatives	238
11.3.2	Other linear molecules	241
11.4	Organogels Based on Banana-Shaped Molecules with AIE	242
11.4.1	Salicylideneaniline derivatives	242
11.4.2	Other banana-shaped gelators	245
11.5	Organogels Based on Dendritic Molecules with AIE	246
11.6	Conclusion	249
	References	250
12	AIE-Active Polymers	253
	<i>Rongrong Hu, Jacky W.Y. Lam and Ben Zhong Tang</i>	
12.1	Introduction	253
12.2	Polyolefins	254
12.3	Polyacetylenes	258
12.4	Polydiynes	259

12.5	Polyarylenes	263
12.6	Polytriazoles	269
12.7	Polysilylenevinylenes	271
12.8	Poly(Vinylene Sulfide)s	272
12.9	Other Systems	277
12.10	Conclusion	280
	References	280
13	Enhanced Emission by Restriction of Molecular Rotation	285
	<i>Jin-Long Hong</i>	
13.1	Background	285
13.2	Strategy to Restrict Molecular Rotation	286
	13.2.1 Introduction of bulky substituents by chemical links	287
	13.2.2 Introduction of bulky groups by complexation	290
	13.2.3 Hindered molecular rotation by hydrogen bonding	292
	13.2.4 Hindered molecular rotation by metal or metal ion chelation	296
13.3	Characterizations of Hindered Molecular Rotations	297
	13.3.1 Solution fluorescence spectroscopy	297
	13.3.2 ¹ H NMR spectroscopy	298
13.4	Conclusion	302
	References	303
14	Restricted Intramolecular Rotations: a Mechanism for Aggregation-Induced Emission	307
	<i>Junwu Chen and Ben Zhong Tang</i>	
14.1	Introduction: 2,3,4,5-Tetraphenylsilole, the Prototype Molecule of Aggregation-Induced Emission (AIE)	307
14.2	Crystal Structures of 2,3,4,5-Tetraphenylsiloles	310
	14.2.1 Twisted arrangements of phenyl groups on the silole core	310
	14.2.2 Enlarged distance between silole cores: far beyond π - π interactions	311
14.3	Restricted Intramolecular Rotation (RIR)	312
	14.3.1 Thickening-enhanced emission of silole solutions (viscchromism)	313
	14.3.2 Piezochromism	313
	14.3.3 Cooling-enhanced emission (thermochromism)	314
	14.3.4 On-off fluorescence switching of silole thin films: activation of rotations in solvent vapors (vapochromism)	316
	14.3.5 Fluorescence decay dynamics	317
	14.3.6 Highly emissive silole solutions: restriction of rotation by internal structural tuning	318
14.4	Conclusion	320
	Acknowledgments	320
	References	320
15	Crystallization-Induced Emission Enhancement	323
	<i>Yongqiang Dong</i>	
15.1	Introduction	323
15.2	Traditional Luminogens	324

15.3	Crystallization-Induced Emission Enhancement (CIEE)	324
15.3.1	CIEE luminogens	325
15.3.2	Potential applications	330
15.4	Conclusion	333
	References	334
16	Time-Resolved Spectroscopic Study of the Aggregation-Induced Emission Mechanism	337
	<i>Bing-rong Gao, Hai-yu Wang, Qi-dai Chen and Hong-bo Sun</i>	
16.1	Introduction	337
16.2	Time-Resolved Spectroscopy	338
16.2.1	Femtosecond time-resolved fluorescence system	338
16.2.2	Femtosecond transient absorption system	339
16.2.3	Time-correlated single-photon counting (TCSPC) system	341
16.3	AIE Molecules Without Electron Donor–Acceptor Units	341
16.3.1	Time-resolved fluorescence study of HPS	341
16.3.2	Time-resolved fluorescence study of CNDPDSB	342
16.3.3	Transient absorption study of CNDPDSB	343
16.4	AIE Molecules with Electron Donor–Acceptor Units	344
16.4.1	Steady-state properties of CNDPASDB	344
16.4.2	Time-resolved fluorescence study of CNDPASDB	346
16.4.3	Transient absorption study of CNDPASDB	351
16.4.4	Discussion	353
16.5	Conclusion	353
	Acknowledgments	354
	References	354
17	Theoretical Understanding of AIE Phenomena Through Computational Chemistry	357
	<i>Qian Peng, Yingli Niu, Qunyan Wu, Xing Gao and Zhigang Shuai</i>	
17.1	Introduction	357
17.2	Fundamental Photophysics Relating to AIE Phenomena	358
17.2.1	Absorption and emission	358
17.2.2	Luminescence quantum efficiency	359
17.3	Computational Approaches to Investigate AIE Molecules	360
17.3.1	Molecular optical spectra formalisms	360
17.3.2	Molecular radiative and nonradiative rate formalisms	365
17.3.3	Computational details	367
17.4	Computational Results	370
17.4.1	Optical spectra	370
17.4.2	Excited-state decay processes	376
17.4.3	A nonadiabatic dynamic simulation	385
17.5	Summary and Outlook	389
	References	390

18	Recent Theoretical Advances in Understanding the Mechanism of Aggregation-Induced Emission for Small Organic Molecules	399
	<i>Jun-Ling Jin, Yun Geng and Zhong-Min Su</i>	
18.1	Introduction	399
18.2	Theoretical Methods	400
	18.2.1 Main photophysical processes of organic molecules	400
	18.2.2 Theoretical estimation of photophysical parameters	402
18.3	Recent Theoretical Advances in Understanding the Mechanism of Aggregation-Induced Emission	406
	18.3.1 Restriction of intramolecular rotation (RIR)	406
	18.3.2 Influence of molecular packing and intermolecular interactions on the photophysical properties and fluorescence efficiencies in the solid phase	411
18.4	Prospects	413
	18.4.1 Other AIE mechanisms except for the conventional RIR mechanism	413
	18.4.2 Design of multifunctional materials with AIE	413
	Acknowledgments	414
	References	414
	<i>Index</i>	<i>419</i>

List of Contributors

Junwu Chen Institute of Polymer Optoelectronic Materials and Devices, State Key Laboratory of Luminescent Materials and Devices, South China University of Technology, China

Qi-dai Chen State Key Laboratory of Integrated Optoelectronics, College of Electronic Science and Engineering, Jilin University, China

Joyce Y. Corey Department of Chemistry and Biochemistry, University of Missouri–St. Louis, USA

Yongqiang Dong Department of Chemistry, Beijing Normal University, China

Suzanne Fery-Forgues Institute of Advanced Technologies in Life Sciences, CNRS ITAV-UMS3039, and Laboratoire IMRCP, CNRS UMR5623, Université de Toulouse, France

Bing-rong Gao State Key Laboratory of Integrated Optoelectronics, College of Electronic Science and Engineering, Jilin University, China

Xing Gao State Key Laboratory of Organic Optoelectronics and Molecular Engineering, Department of Chemistry, Tsinghua University, China

Yun Geng Institute of Functional Materials Chemistry, Faculty of Chemistry, Northeast Normal University, China

Mina Han Department of Molecular Design and Engineering, Nagoya University, Japan

Jin-Long Hong Department of Materials and Optoelectronic Science, National Sun Yat-Sen University, Taiwan

Rongrong Hu Department of Chemistry, The Hong Kong University of Science and Technology, China

Jianli Hua Key Laboratory for Advanced Materials and Institute of Fine Chemicals, East China University of Science and Technology, China

Jing Huang Department of Chemistry, Wuhan University, China

Jun-Ling Jin Institute of Functional Material Chemistry, Faculty of Chemistry, Northeast Normal University, China

Jacky W.Y. Lam Department of Chemistry, The Hong Kong University of Science and Technology, China

Qianqian Li Department of Chemistry, Wuhan University, China

Zhen Li Department of Chemistry, Wuhan University, China

Ran Lu State Key Laboratory of Supramolecular Structure and Materials, College of Chemistry, Jilin University, China

Jerome L. Mullin Department of Chemistry and Physics, University of New England, USA

Yingli Niu State Key Laboratory of Organic Solids, Beijing National Laboratory for Molecular Science, Institute of Chemistry, Chinese Academy of Sciences, China

Yasuo Norikane Electronics and Photonics Research Institute, National Institute of Advanced Industrial Science and Technology (AIST), Japan

Qian Peng State Key Laboratory of Organic Solids, Beijing National Laboratory for Molecular Science, Institute of Chemistry, Chinese Academy of Sciences, China

Anjun Qin MOE Key Laboratory of Macromolecule Synthesis and Functionalization, Department of Polymer Science and Engineering, Zhejiang University, China

Xiao Yuan Shen MOE Key Laboratory of Macromolecule Synthesis and Functionalization, Department of Polymer Science and Engineering, Zhejiang University, China

Masaki Shimizu Department of Biomolecular Engineering, Graduate School of Science and Technology, Kyoto Institute of Technology, Japan

Zhigang Shuai State Key Laboratory of Organic Optoelectronics and Molecular Engineering, Department of Chemistry, Tsinghua University, China

Zhong-Min Su Institute of Functional Materials Chemistry, Faculty of Chemistry, Northeast Normal University, China

Hong-bo Sun State Key Laboratory of Integrated Optoelectronics, College of Electronic Science and Engineering, Jilin University, China

Jing Zhi Sun MOE Key Laboratory of Macromolecule Synthesis and Functionalization, Department of Polymer Science and Engineering, Zhejiang University, China

Ben Zhong Tang Department of Chemistry, Institute of Molecular Functional Materials, The Hong Kong University of Science and Technology, and Institute of Polymer Optoelectronic Materials and Devices, State Key Laboratory of Luminescent Materials and Devices, South China University of Technology, China

He Tian State Key Laboratory for Advanced Materials and Institute of Fine Chemicals, East China University of Science and Technology, China

Wenjing Tian State Key Laboratory of Supramolecular Structure and Materials, Jilin University, China

Henry J. Tracy Department of Chemistry, University of Southern Maine, USA

Hai-yu Wang State Key Laboratory of Integrated Optoelectronics, College of Electronic Science and Engineering, Jilin University, China

Yue Wang State Key Laboratory of Supramolecular Structure and Materials, College of Chemistry, Jilin University, China

Qunyan Wu State Key Laboratory of Organic Optoelectronics and Molecular Engineering, Department of Chemistry, Tsinghua University, China

Bin Xu State Key Laboratory of Supramolecular Structure and Materials, Jilin University, China

Pengchong Xue State Key Laboratory of Supramolecular Structure and Materials, College of Chemistry, Jilin University, China

Hao Zhang State Key Laboratory for Advanced Materials and Institute of Fine Chemicals, East China University of Science and Technology, China

Hongyu Zhang State Key Laboratory of Supramolecular Structure and Materials, College of Chemistry, Jilin University, China

Jibo Zhang State Key Laboratory of Supramolecular Structure and Materials, Jilin University, China

Preface

The discovery of new natural phenomena, the unveiling of new physical laws, the development of new methodologies, and the generation of new knowledge are at the core of scientific research. From this viewpoint, the study of light-emitting behaviors of luminogens in an aggregate state is a challenging yet important topic because it may lead to the creation of new photophysical knowledge.

Since the 1950s, studies have shown that the fluorescence of a number of luminophores became weaker or even completely quenched in concentrated solutions or in the solid state. This common photophysical phenomenon is widely known as ‘concentration quenching’ or ‘aggregation-caused quenching’ (ACQ) of light emission. The ACQ process has been studied in great detail, and mature theories have been established. The ACQ effect, however, is harmful in practice, because luminophores are usually used as solid films or aggregates in real-world applications, which hinders them from realizing their full potential. Numerous processes have been employed and many approaches have been developed to prevent the luminophores from aggregating, but these efforts have met with only limited success. The difficulty lies in the fact that chromophore aggregation is an intrinsic natural process when luminophore molecules are located in close vicinity in the condensed phase.

Exactly opposite to the ACQ effect, in 2001 we observed a unique luminogen system in which aggregation played a constructive, instead of destructive, role in the luminescence process: a molecule named 1-methyl-1,2,3,4,5-pentaphenylsilole was found to be almost nonemissive in dilute acetonitrile solution but became highly fluorescent when a large amount of water was admixed with acetonitrile. Because water is a poor solvent of the hydrophobic silole luminogen, addition of water to acetonitrile causes the silole molecules to aggregate in aqueous media. As the light emission is induced by aggregate formation, we coined the term *aggregation-induced emission* (AIE) for the phenomenon. In the past decade, a large variety of molecules with propeller shapes have been found to show the AIE effect, indicating that AIE is a general, rather than special, photophysical phenomenon.

On the basis of our experimental results, we have rationalized that the restriction of intramolecular rotation (RIR) is the main cause of the AIE phenomenon. In the solution state, intramolecular rotation of the aromatic rotors of the AIE luminogens is active, which serves as a relaxation channel for the excited states to decay nonradiatively. In the aggregate state, however, the intramolecular rotation is restricted owing to the physical constraint involved, which blocks the nonradiative pathway and opens the radiative channel.

The novel AIE phenomenon offers a new platform for researchers to look into the light-emitting processes from luminogen aggregates, from which useful information on structure–property relationships may be collected and mechanistic insights may be gained. Such information and insights will be instructive to the structural design for the development of new efficient AIE luminogens. Furthermore, the discovery of the AIE effect overturns the general belief of ‘concentration quenching’ or ACQ of luminescence processes, opens a new avenue for the development of new luminogen materials in the aggregate or solid state and may spawn new models or theorems for photophysical processes in solution and aggregate states.

As AIE is a photophysical effect concerning light emission in the practically useful solid state, AIE studies may also lead to hitherto impossible technological innovations. In AIE systems, one can take great advantage of aggregate formation, instead of fighting against it. The AIE effect permits the use of highly concentrated solutions of luminogens and their aggregates in aqueous media for sensing and imaging applications, which may lead to the development of fluorescence turn-on or light-up nanoprobes. A probe based on AIE luminogen nanoaggregates is in some sense the organic version of inorganic semiconductor quantum dots, but are superior to the latter in terms of wider molecular diversity, readier structural tunability, and better biological compatibility.

Attracted by this intriguing phenomenon and its promising applications, a number of research groups throughout the world have enthusiastically engaged in AIE studies, and exciting progress has already been made. In response to an invitation from the Wiley editors, we embarked on the preparation of two volumes dedicated to the study of AIE – this volume, *Aggregation-Induced Emission: Fundamentals* and the related volume, *Aggregation-Induced Emission: Applications*.

In this volume, we invited a group of active researchers in the area to contribute on the fundamental issues of the study of AIE. These include the design, synthesis, and photophysical behavior of AIE-active molecules and polymers. The control of the morphological structures of the aggregates of the AIE-active materials and the experimental investigation and theoretic understanding of the RIR process or the AIE mechanism are also covered in this volume.

This book is expected to be a valuable reference to readers who are now working or planning to be involved in the areas of research on organic optoelectronic materials and biomedical sensors. Although we have tried our best to make this book comprehensive, some important work may have inadvertently been omitted, owing to the limitations on the size of the book and the rapid developments in this area of research. The book may contain some overlapping contents in different chapters and possibly even some errors. We hope the readers will provide us with constructive comments, so that we may modify and improve the book in its next edition.

We would like to thank all the authors who have contributed to this book. Without their enthusiastic support, the foundation of this book could not have been laid. We also thank the Wiley in-house editors, Sarah Hall, Sarah Tilley, and Rebecca Ralf, for their enthusiastic encouragement and technical support. We hope that this book will serve as a ‘catalyst’ to stimulate new efforts, to trigger new ideas, and to accelerate the pace in the research endeavors on the design of new AIE luminogen systems, the establishment of new theoretical models, and the exploration of innovative applications.

Anjun Qin

Department of Polymer Science and Engineering
Zhejiang University, China

Ben Zhong Tang

Department of Chemistry, Division of Biomedical Engineering
The Hong Kong University of Science and Technology
China

1

Synthesis of Siloles (and Germoles) that Exhibit the AIE Effect

Joyce Y. Corey

Department of Chemistry and Biochemistry, University of Missouri–St. Louis, USA

1.1 Introduction

As reported in 2001 by Tang and co-workers [1], the identification of the aggregation-induced emission (AIE) effect was intimately connected with a study of siloles and stemmed from the simple observation that a wet spot containing 1-methyl-1,2,3,4,5-pentaphenylsilole ($\text{Ph}_4\text{C}_4\text{SiMePh}$) (MPS) on a thin-layer chromatographic (TLC) plate barely fluoresced under UV light but was clearly visible when the spot dried. In contrast to the expectation of the time period that in the solid state aggregation would cause quenching [aggregation-caused quenching (ACQ)] of the photoluminescence (PL) processes of luminophoric molecules, the silole exhibited the reverse behavior: a sample was virtually nonfluorescent in solution but fluorescent in the solid state. For applications in electronic devices, thin films of a luminophoric material are required and the appearance of ACQ would thus inhibit such applications. An electroluminescent (EL) device was constructed with MPS and was demonstrated to be a good light-emitting material for device applications [1]. The observation of AIE in siloles was not the beginning of the search for siloles that could be efficiently incorporated into organic light-emitting diodes (OLEDs), as Tamao *et al.* had demonstrated in 1996 that siloles were efficient electron-transporting materials and showed that the device performance was related to the substituents in the 2,5-positions of the ring [2]. This was actually the first demonstration that siloles could be good candidates as core components for organic EL devices. The AIE luminogens, however, have additional applications, for example, as chemical sensors, biological probes, and smart nanomaterials. The ‘turn-on/light-up’ nature of an AIE sensor makes for ready use in the field or for on-sight screening, to name just a couple of applications, which will be highlighted in other chapters.

2 Aggregation-Induced Emission: Fundamentals

This chapter focuses on the synthetic methods that have been used to target silacyclopentadiene and germacyclopentadiene derivatives (common names: silole and germole) and their related benzene-annulated derivatives. Synthetic examples that have actually been described as exhibiting the AIE effect will be discussed whenever possible. However, silole systems have been studied since the first report in 1959 by Braye and Hübel of the formation of $\text{Ph}_4\text{C}_4\text{SiPh}_2$ (HPS), presumably by a rather obscure synthesis from reaction of $\text{Fe}_2(\text{CO})_6(\text{PhC}_2\text{Ph})_2$ with Ph_2SiCl_2 , and related to that which was used to produce pentaphenylphosphole from the same iron precursor and PhPCl_2 [3a]. The same group subsequently described a better method for the synthesis of HPS [3b] that is still in use today and is the first method that will be described in Section 1.3.1. The material covered will not provide a comprehensive listing of all systems that have been prepared but will attempt to describe the methodology that has been developed for targeting the silole core, illustrated with selected examples. Since three of the principal methods for silole formation predate the discovery of the AIE effect, testing for this phenomenon has understandably not been reported in publications prior to 2001. One of the more interesting examples was the first viable synthesis of HPS (in 1961), where it was stated: ‘In the solid state it exhibits a strong blue fluorescence in ultraviolet light . . .’ [3b]. It is this solid-state fluorescence that has become a feature of the AIE effect and proves once again that ‘chance favors the prepared mind’ in its discovery.

The rest of this chapter is divided into the following sections. Section 1.2 contains background material on the nomenclature of siloles and their benzene-annulated relatives and the numbering systems that are commonly used and that will be utilized in this chapter. A brief introduction to the bond formation methods in silicon chemistry that are relevant to the formation of siloles will be included, as this type of chemistry imposes certain limitations on how the synthesis of a particular silole might be approached. In general, it is the role of organic chemistry in forming the carbon portion of siloles and their related derivatives that has actually enabled the presence of various substitution patterns to be incorporated into the target metallacycle. This is seen particularly in the Tamao synthesis (Section 1.3.2) of siloles and in the formation of precursors to the benzene-annulated systems (Section 1.6.2). The substitution reactions possible at both the silicon center and the carbon centers of the metallacycle also play a role, particularly in the area of copolymer synthesis. Lastly, Section 1.2 gives brief comments on the early calculations for the HOMO and LUMO energy levels for siloles as compared with the related carbon parent and the heterocycles of N and S.

Section 1.3 contains the bulk of the synthetic chemistry and describes three basic approaches to siloles as well as the more recent methodology that involves the use of transition metals both stoichiometrically (early work) and catalytically. Section 1.4 covers methods that can be used to modify the silole core and 1.5 addresses whether the synthetic methods can be extended to the heavier Group 14 element, germanium. Section 1.6 will describe basic routes to silaindenes and silafluorenes that are related to those used for siloles. Section 1.7 contains a brief discussion on the extension to oligomers and both homo- and copolymers that contain a silicon or germanium metallole, metallaindene, and metallafluorene. The last section contains a summary and commentary on future directions.

1.2 Background

The numbering scheme for siloles and the benzene-annulated derivatives is illustrated in Figure 1.1. The silaindenes are sometimes referred to as benzosiloles and the silafluorenes as dibenzosiloles, but the first name listed will be used in this chapter. The silaindene shown is technically *1H*-1-silaindene and the silafluorene is *9H*-9-silafluorene, but the *1H* and *9H* are often omitted. The germanium analogs are similarly numbered and named (germaindenes and germafluorenes).

Probably the limiting factor in the assembly of the systems shown in Figure 1.1 is the small number of C—Si bond formation methods. One of the two general methods involves a salt metathesis reaction of an

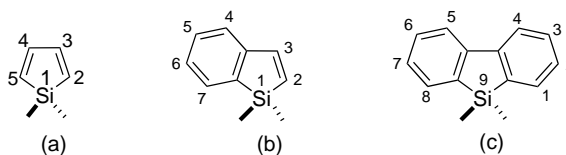


Figure 1.1 Skeleton structures with positions numbered. (a) Siloles; (b) 1-silaindenes (benzosiloles); (c) silafluorenes (dibenzosiloles).

organolithium or organoGrignard reagent with a silicon halide (elimination of a metal halide). The second is addition of an Si—H bond to an unsaturated organic substrate, $>\text{C}=\text{C}<$ or $-\text{C}\equiv\text{C}-$. Such a reaction is referred to as hydrosilylation and is commonly initiated with a transition metal catalyst. Nucleophilic substitutions at silicon dominate organosilicon chemistry. From an organic chemist's perspective, organosilicon chemistry is currently a matter of manipulation of single bonds. Although compounds that contain an $\text{Si}=\text{X}$ unit ($\text{X} = \text{C}, \text{Si}, \text{N}, \text{P}$, transition metal) are known, their practical use in synthesis awaits future development. An exception to these general observations is the recently published transition metal-promoted reactions that can involve $\text{SiH}-\text{HC}$ coupling for ring closure.

Simple calculations (*ab initio*) performed for the model silole $\text{H}_4\text{C}_4\text{SiH}_2$ with a comparison with the parent carbon system, $\text{H}_4\text{C}_4\text{CH}_2$, and the sulfur heterocycle, $\text{H}_4\text{C}_4\text{S}$, and also a series of N heterocycles demonstrated that the silole had the lowest HOMO–LUMO energy gap in addition to a low-lying LUMO level [2, 4]. The low-lying LUMO level was attributed to efficient $\sigma^*-\pi^*$ overlap from the σ^* orbital associated with the exocyclic σ -bonded substituents on the silicon center and the π^* orbital of the butadiene unit. No such orbital is available for the parent carbon species or for the other five-membered heterocycles (with N, O or S heteroatoms). However, model systems, although simpler to calculate, do not reveal the role that substituents may play in the relative energies of the HOMO and LUMO, nor do they indicate substituent variations that might lead to better electron-transporting (ET) materials. Marder and co-workers summarized the effects of substituents on the electronic structure of siloles, including the physical data that support the trends that illustrate the importance of substituents and their location on the silole core [5]. Yamaguchi and Tamao also briefly reviewed the role of orbital interactions in main group element-containing π -electron systems, heteroles, dibenzoheteroles, and element-bridged stilbenes, although the focus was on boron and silicon heteroatoms [6].

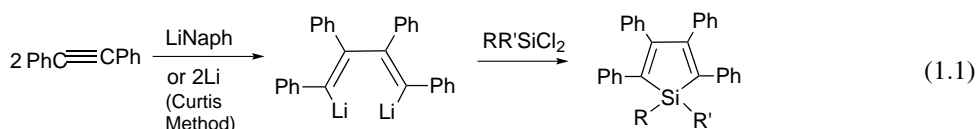
Although the synthesis reported for HPS in 1961 [3b] is still in use today, other approaches have been developed especially since the 1990s. What becomes useful to an individual investigator will depend on the substitution pattern desired either on the carbon backbone or the silicon center. Two fundamental strategies are possible, one in which the carbon core is constructed and then connected to the heteroatom, and the other where the substituents are added to the silicon center and then C—C bond formation between two of the substituents is initiated. In either case, a common precursor will be an alkyne or diyne even when the C—C bond is formed between two of the silicon substituents. Transition metal-catalyzed formation of siloles (and their benzene-annulated derivatives) is of relatively recent origin and the actual ring formation details will vary depending on the catalyst. As will be seen, the most commonly prepared siloles have substituents on all (four) carbons, but this will not be the case for either silaindenes or silafluorenes. In fact, methods to obtain substituted precursors to silafluorenes are actually relatively recent. In Section 1.3 the synthetic methods will be introduced in the following order: Section 1.3.1, reductive dimerization of 1,2-diaryllkynes; Section 1.3.2, intramolecular reductive cyclization of dialkynylsilanes; Section 1.3.3, 1,1-organoboration of dialkynylsilanes; and Section 1.3.4, transition metals in silole formation. Modifications that utilize preformed siloles to include a desired C or Si substituent are the subject of Section 1.4.

1.3 Synthesis of Siloles

There have been several general reviews of the synthesis of main group heterocycles or heterocycles of silicon (with varying ring sizes) [7] and others that involve only siloles and related compounds [8]. Additional reviews that are more narrowly focused will be mentioned where the particular synthetic method is described.

1.3.1 Reductive dimerization of tolan

Historically, the first practical method for the formation of siloles involved a ring closure at a silicon center by a metathesis reaction of a dilithio reagent generated from Li and $\text{PhC}\equiv\text{CPh}$ (tolan) with Ph_2SiCl_2 to give HPS in 50% yield. Subsequently, this synthetic approach has often been referred to as the Curtis method (Equation 1.1).



The reductive dimerization of tolan (diphenylacetylene) with Li metal or LiNaph (lithium naphthalenide) results from the transfer of an electron to PhC_2Ph to produce a radical anion that dimerizes to give the dianion, 1,4-dilithio-1,2,3,4-tetraphenylbutadiene [9a]. An ethereal solution from the reaction of Li and PhC_2Ph develops a deep red color and deposits a red precipitate, which, when quenched with water, gives 1,2,3,4-tetraphenylbutadiene. However, if the solution turned brown (with a brown precipitate), aqueous quenching provided 1,2,3-triphenylnaphthalene and seemed to occur when excess metal was present [9a]. The color change signifies ‘death’ from the standpoint of the potential generation of a silole and, unfortunately, the trigger for this catastrophic rearrangement is unknown. Braye *et al.* commented on the problem in the first practical synthesis of HPS and suggested that the reaction time should be limited and that working on a larger scale could suppress the rearrangement [3b]. In contrast to early recommendations that the stoichiometry for the reaction of $\text{PhC}\equiv\text{CPh}$ with Li (or LiNaph) be held at 1:2, various investigators have used acetylene-to-Li ratios ranging from 0.2:1 to 2:1 and have achieved modest yields that generally lay between 40 and 70% after reaction with an appropriate chlorosilane [8c]. A variety of dichlorosilanes have been used as the quenching agent, including the types R_2SiCl_2 (such as $\text{R} = \text{Ph}, \text{Me}$), RR'SiCl_2 ($\text{R}, \text{R}' = \text{PhMe}$), and also the chlorosilanes HSiCl_3 and SiCl_4 . With HSiCl_3 , the silole produced is $\text{Ph}_4\text{C}_4\text{SiHCl}$, which has two functional groups on silicon that can be substituted by different types of reactions: salt metathesis of $\text{Si}-\text{Cl}$ to incorporate mainly an organic substituent and hydrosilylation of multiple bonds with HSi . With SiCl_4 , the product is $\text{Ph}_4\text{C}_4\text{SiCl}_2$. One of the more interesting tactics in trying to control the degradation of the dilithiobutadiene was through monitoring the reaction for the presence of butadiene in hydrolyzed aliquots of the reaction mixture by gas chromatography (GC), then freezing in liquid N_2 . In this case, the SiCl_4 is layered over the solidified reaction mixture, then warmed slowly to room temperature. The yield of isolated $\text{Ph}_4\text{C}_4\text{SiCl}_2$ was 50–70% [9b,c]. Because the range of commercially available dichlorosilanes is not large, $\text{Ph}_4\text{C}_4\text{SiCl}_2$ is often generated *in situ* and then treated with organometallic reagents such as $\text{LiC}_6\text{H}_4\text{CH}_2\text{NET}_2\text{-}p$ [10], $\text{C}_6\text{F}_5\text{MgBr}$ [11], and several other cases listed in [8c]. This same tactic of generating the functional silole *in situ* by quenching with HSiCl_3 followed by an organometallic reagent has also provided several examples of $\text{Ph}_4\text{C}_4\text{SiHR}$ [8c].

The reductive dimerization of $\text{ArC}\equiv\text{CAr}$ has almost exclusively been performed for $\text{Ar} = \text{Ph}$, although there is one example where $\text{Ar} = 9,9\text{-dimethylfluoren-2-yl}$ [12]. It is certainly likely that substituted

aromatic rings such as $-\text{C}_6\text{H}_4\text{X}$ (X in a *meta* or *para* position) could be utilized, but such experiments do not seem to have been reported in the literature. The reductive dimerization of $\text{PhC}\equiv\text{CAr}$ is more problematic as three silole isomers could be formed: 2,4-diphenyl, 2,5-diphenyl, and 3,4-diphenylsilole. One of the more interesting cases reported recently was the reaction utilizing $\text{PhC}\equiv\text{CAr}$, $\text{Ar} = 2,6\text{-diisopropylphenyl}$, where the silole_{2,4}:silole_{2,5}:silole_{3,4} ratio was found to be 40:2.3:1, with the most sterically hindered silole (i.e. with the two diisopropylphenyl substituents on adjacent positions) formed in the least amount. In what must be a real *tour de force* effort, the three isomers were isolated after 20 chromatographic separations [13]. Calculations were reported for $\text{C}_4\text{Ph}_4\text{SiMe}_2$ and $\text{C}_4\text{Ph}_2\text{Ar}_2\text{SiMe}_2$ [$\text{Ar} = 3,4\text{-bis}(2,6\text{-diisopropylphenyl})$] about a year later [14]. The calculations showed that the twisting motions of the phenyl groups in the 3,4-positions dissipate the excited-state energy nonradiatively. The presence of the bulky 2,6-diisopropyl groups on the phenyl rings in the 3,4-positions completely suppressed this channel for loss of energy, resulting in enhanced PL [14].

Although the AIE effect was first identified in 2001 [15] by Tang and co-workers during a study of the properties 1-methyl-1,2,3,4,5-pentaphenylsilole (MPPS), it could just as well have been HPS that was the subject of a report by Tang's group published about a month later [16]. Historically it is HPS that was the first silole that was reported and has subsequently become a 'poster child' for silole chemistry. HPS has been widely studied since the end of the 1990s in terms of physical measurements that have been reported in at least 15 publications (about half of which are from Tang's group). Three papers contain synthetic details, with minor experimental differences, for the preparation of HPS utilizing $\text{PhC}\equiv\text{CPh}$ and Li followed by addition of Ph_2SiCl_2 ($\text{PhC}\equiv\text{CPh}:\text{Li}$, %: 1:1, 44% [17]; 1:2, 68% [16]; 1.05:1, 60% [18]), and all give spectroscopic data including PL measurements and activation energies. The X-ray structure has also been determined [19, 20], Electrochemical properties have been reported for HPS from cyclic voltammetric (CV) measurements [17] and also photoelectron spectroscopy (PES) and inverse photoelectron spectroscopy (IPES) data, including density functional theory (DFT) calculations. Calculations have also been reported including equilibrium geometries (MO) [17], excitation energies [time-dependent density functional theory (TD-DFT)] [21], excited-state properties (DFT methods) [22], carrier transport properties (Hartree-Fock and DFT) [23] and calculated structures to compare with experimental structures (DFT Dmol3 package) [24]. Electron mobility in films has been measured and that of the HPS was ~ 1.5 times higher than that of an MPPS film, hence it has better ET properties in a light-emitting diode (LED). HPS also has a higher mobility than that of Alq_3 [tris(8-hydroxyquinolinato)aluminum], a widely used electron transport material [24].

A desirable feature for an OLED device is a high PL quantum yield (Φ_{PL}) in the solid state. The quantum yield for various siloles has certainly been reported, but at this point only the results for HPS will be described. The value of Φ_{PL} is determined by comparison with a standard, although the choice of standard is not uniform for all studies. The solution Φ_{PL} is a function of the solvent and, for solids, the particular phase (different solid forms). The solution Φ_{PL} has been measured in six solvents (in the same study) with values that are low in all five solvents in which HPS is soluble (insoluble in EtOH) and follows the order dioxane $>$ C_6H_6 $>$ THF $>$ CH_2Cl_2 $>$ CH_3CN , with values varying from 0.42 to 0.09% [20]. The Φ_{PL} values for HPS as an average over the solvents was 0.21%, for the solution aggregates from dioxane–water 38% and for an SOA (sucrose octaacetate) glass containing HPS 59% [20]. The enhancement of the value of Φ_{PL} of HPS on SOA glass over its solution value in dioxane was 140-fold.

The Φ_{PL} for HPS crystalline films, amorphous films, and nanowires with various diameters has been reported with accompanying time-dependent fluorescence measurements. The results indicate that the excited states of HPS decay through a fast and a slow pathway. In crystalline HPS ($\Phi_{\text{PL}} = 86\%$), 94% of the molecules decay through a slow pathway (6% by the fast pathway). In the amorphous form ($\Phi_{\text{PL}} = 78\%$), 75% of the molecules decay by the slower pathway. The nanowires decay by an increasing extent through the faster pathway as the diameter of the nanowire increases in increments from 35 nm (14%) to 250 nm

(21%). It was concluded that the fast-pathway decay contributes little to the emission spectra whereas the relaxation of the excited states dominates the slower deactivation process [25]. In another study, the Φ_{PL} value for HPS was determined in cyclohexane to be 0.30% and in a thin film 78%, which is a 260-fold enhancement from solution to the solid, and with the corresponding $\text{Ph}_4\text{C}_4\text{SiPhMe}$ that enhancement was 654-fold [24].

When a silole is dissolved in a ‘good’ solvent, PL is very weak. However, once a large amount of water (a ‘poor’ solvent) is added, intense PL spectra are obtained. The siloles aggregate with higher water content, and since there is no observable precipitate, nanoparticles were suspected to be the source of the PL [15]. The size distribution of the nanoparticles formed from HPS in water–acetone mixtures at 70 and 90% volume fractions of water exhibited average particle sizes of ~ 53 and ~ 82 nm, respectively. In this study, the AIE effect (enhanced emission in the solid state) was attributed to restricted intramolecular rotation (RIR) of the phenyl rotors around the single bonds that link them to the core of the silole [19].

The AIE effect for nanoparticles has been explored in several applications, a few of which are described here. A ball-milling process was used to obtain nanocrystalline HPS, which was encapsulated in thin polyelectrolyte layers that then provided an ‘interface’ for the attachment of antibodies through adsorption at the interface. The usual quenching problem arising for the ratio of fluorescent dyes to biomolecules (F:P ratio = 2.4×10^{-3}) is prevented by the AIE property of the silole. The fluorescence signal from the nanocrystalline siloles was 40–140-fold higher in an M IgG assay compared with direct FITC-labeled antibodies [26]. The isolation of HPS nanostructures from THF by addition of water along with attendant (SEM) images for those isolated from 60, 70, 80, and 90% water illustrated the changes in morphology of the nanoparticles and included nanoflowers at 70% water, nanoglobules mixed with nanoflowers at 80% and microglobules at 90%. The various types exhibited enhanced and color-tunable photophysical properties. The nanoflowers produced in 70% water in THF exhibited a 100-fold increase in intensity relative to the emission for dilute THF solutions. Time-resolved fluorescence data gave a mean lifetime of 4.6 ns for the nanoflowers and a fluorescence quantum efficiency of 35% [27]. Nanowires of HPS with tunable PL have also been reported when nanoporous alumina membranes were immersed in a saturated solution of the silole. Nanowires with different diameters were observed and characterized, in part, by SEM images and also by X-ray diffraction (XRD). HPS aggregates have also been incorporated into a chitosan film where the fluorescence emission is stable and selective for the presence of picric acid with a detection limit of $\sim 2 \times 10^{-8} \text{ mol l}^{-1}$. Related compounds such as trinitrotoluene (TNT), dinitrotoluene (DNT), and nitrobenzene (and others) had no effect on the fluorescence emission of the field [18].

The vapochromism of HPS absorbed on a TLC plate was reported since a sample of HPS fluoresces when dry but not when exposed to solvent vapor, and this ‘off’ and ‘on’ behavior was reversible. If the film is formed on a quartz surface, a change from a green fluorophore to a blue emitter takes place after exposure to solvent and is not reversible. The SEM and TEM images of the film before and after exposure to acetone clearly show a transformation from an amorphous phase (before) to a crystalline phase (after) [28]. In a similar type of experiment, HPS thin films were prepared by spin coating and subjected to solvent fuming and the results of solvent annealing were monitored by SEM images. When the film was subjected to methanol annealing, nanobelts, and nanorods were observed, but after benzene vapor annealing the nanoparticles disappeared and an amorphous HPS film was observed. Annealing with isopropyl alcohol vapor followed by chlorobenzene vapor annealing revealed the same sequence as did acetone vapor annealing followed by THF vapor annealing. The SEM images provide convincing evidence for the crystal formation [29]. Although SEM images may be the most helpful in determining morphologies of crystalline solids, there is some support for the use of Fourier transform infrared (FTIR) spectra in demonstrating crystal powders versus amorphous powders, although this was demonstrated not for HPS but for 1,1-bis(2'-thienyl)-2,3,4,5-tetraphenylsilole [30].

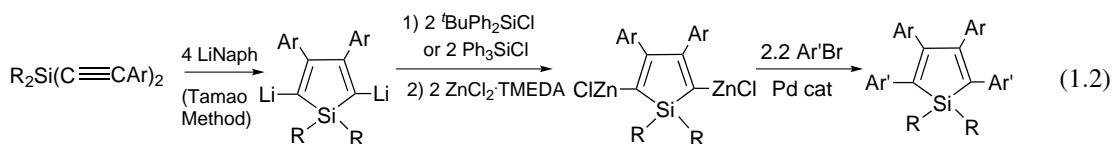
The previous paragraph gives only a hint of the applications of the AIE effect in siloles. There are siloles that are prepared by other methods, primarily the Tamao procedure (covered in the next section), and by

appropriate substitution reactions at silicon (described in Section 1.4.1). For a more extensive discussion of applications that include siloles, see the reviews on luminogenic materials with AIE [31a], a brief account of the Tang group's development of the AIE mechanism and applications [31b], and AIE in both silole molecules and polymers where other researchers' efforts are included [31c].

Before leaving this section, the strengths and weaknesses of the Curtis method should be mentioned. The reaction involves the use of tolan, a commercially available material that automatically places phenyl substituents on each of the carbon atoms of the silole core. The reaction is not practical for unsymmetrically substituted alkynes ($\text{ArC}\equiv\text{CAr}'$) as three silole isomers can form, and it also cannot be used for alkynes with alkyl or silyl substituents (these will be incorporated later in another method). The synthetic approach can be used to ring close at silicon with a variety of chlorosilanes with two or more Cl substituents. Although the carbon core substituents are not varied, those at the silicon center (1,1-position) are readily varied through standard nucleophilic substitutions of an SiCl bond or reaction of an SiH bond with a multiple bond. The next section describes the synthesis of siloles where the 2,5-substituents may differ from the 3,4-substituents.

1.3.2 Intramolecular cyclization of dialkynylsilanes

A completely new approach to silole formation was introduced by Tamao and co-workers in 1994. In this method, two alkynyl groups tethered to silicon are cyclized by reductive coupling of two carbon centers using LiNaph (or Li) as the reductant. The ring closure reaction places two anionic centers on the carbons α to the Si center, thus permitting the introduction of substituents either through salt metathesis with a silicon halide or ultimately by a cross-coupling reaction (Equation 1.2). Yamaguchi and Tamao summarized the early work on this new silole-forming method [32] and on the role of cross-coupling of silole monomers in oligomer and polymer formation [33].



The Tamao 'one-pot' approach to siloles has become the most popular method for the generation of siloles, although it does require the synthesis of the appropriate dialkynylsilane precursors as these are not commercially available. Although some details of the method appeared in a paper on oligosiloles [34a] in 1994, a full paper describing the procedure for monomeric siloles was not published until 2000 and provided the details for the isolation of 17 siloles from $\text{Me}_2\text{Si}(\text{C}\equiv\text{CPh})_2$ [34b]. The reaction method requires simultaneous reduction of the carbon atoms of the alkyne β to the Si center followed by the coupling of the two radical centers to form a C—C bond and closing the ring. Not surprisingly, an aryl substituent is required on the β -carbon, as the precursors such as $\text{R}_2\text{Si}(\text{C}\equiv\text{CR}')_2$ where $\text{R}' = \text{alkyl or silyl}$ give complex mixtures of products from the reduction. Although the intermediate dilithiosilole that is formed can be quenched with a simple reagent such as MeI [35], the more common route is to treat the dilithiosilole with ZnCl_2 (or $\text{ZnCl}_2\text{-tmeda}$) to form the 2,5-ZnCl-substituted silole *in situ*, which is then cross-coupled with an aromatic bromide utilizing $\text{Pd}(\text{PPh}_3)_4$ or $\text{PdCl}_2(\text{PPh}_3)_2$ as the catalyst. A second cross-coupling route utilizes the reaction of the 2,5-ZnCl substituents with Br_2 or *N*-bromosuccinimide (NBS) to give a 2,5-dibromosilole, which may or may not be isolated [36]. Isolation of three dibromides with different sets of substituents at the 1,1-position (Me_2 , MePh , Ph_2) [37] was recently reported and earlier, isolation of three dibromides of $\text{Ph}_2\text{Br}_2\text{C}_4\text{SiR}_2$ where $\text{R} = \text{Et}$, ^iPr , Hex was described [34a]. A very detailed account of the

preparation of 2,5-dibromo-1,1-dimethyl-3,4-diphenyl-1*H*-silole was published in *Organic Synthesis* [38]. The 2,5-dibromosilole is useful for cross-coupling reactions (particularly with terminal alkynes [37, 39]). Reaction conditions for the lithiation of one of the two bromides to give the intermediate monolithio intermediate ($\text{Ph}_2\text{BrLiC}_4\text{SiEt}_2$) was reported by Tamao *et al.* [34a]. Quenching of the lithio reagent with ClSnBu_3 gave $\text{Ph}_2\text{Br}(\text{SnBu}_3)\text{SiEt}_2$ and thus produced a silole that has two different groups that can react under different cross-coupling conditions [34a]. A second variation, reported by Pagenkopf and co-workers, was the treatment of the 2,5-dilithiosilole intermediate with *N*-chlorophthalimide followed by iodine, which provided the asymmetrically substituted 2-chloro-5-iodosilole [39]. This also then allows two different cross-coupling reactions to be performed, leading to two different substituents at the 2,5-positions, and was exploited by Pagenkopf and co-workers to introduce an electron-donating substituent at one of the positions and an electron-accepting substituent at the remaining position [39]. A listing of siloles prepared by the Tamao procedure can be found in [8c]. An important feature in the improvement of the yields for this method was the addition of a bulky silane (Ph_3SiCl) or excess $\text{ZnCl}_2 \cdot \text{tmeda}$ (4 equivalents) to the intermediate dilithiosilole to quench any excess LiNaph used for the reductive coupling step [34b].

In contrast to the Curtis method (Section 1.3.1), the original Tamao procedure could not be used for silole precursors such as $\text{Cl}_2\text{Si}(\text{C}\equiv\text{CPh})_2$. However, a route to mono- and difunctional siloles was developed utilizing $(\text{Et}_2\text{N})_2\text{SiCl}_2$ (formed from SiCl_4 and 2 molar equivalents each of Et_2NH and Et_3N) to obtain the precursor, $(\text{Et}_2\text{N})_2\text{Si}(\text{C}\equiv\text{CPh})_2$ [40]. The successful conditions for the reductive coupling involved addition of the diethynylsilane to an excess of LiNaph at -78°C to form the 2,5-dilithio-1,1-diaminosilole. Trapping with Me_3SiCl or dimethyl sulfate gave the 2,5-bis(trimethylsilyl)- and 2,5-dimethylsiloles in 83 and 70% isolated yields, respectively [40]. Both $\text{Et}_2\text{N}-$ groups of both siloles could be converted to a difunctional silole with alkoxy or chloro groups. The latter conversion is an indirect route to dichlorosiloles, which could then be converted to a variety of 1,1-diorganosiloles as also described in Section 1.3.1. It should be noted that all the siloles with 2,5-methyl substituents were unstable in air.

There are many examples of different substituents that have been incorporated into the 2,5-positions and a few examples are shown in Figure 1.2. After the demonstration by Tamao's group that siloles could function as core components in ET materials, including systems where the 2,5-aryl groups have been modified, various research groups have tried to improve the quantum yields of the siloles and to obtain a range of colors from the emission (see [8c] for the variations). Just as the siloles prepared by the Curtis method were weak emitters in solution, so also are the various siloles prepared by the Tamao procedure. In an earlier review of the effects of substituent locations on the electronic structure of the siloles by Marder and co-workers [5], it was argued that the largest effects were exerted by the 2,5-substituents and that these have the greatest potential to alter the optical properties, especially if there are strong π -interactions of the substituents with the silole core [5]. Since in applications in electronic devices the silole is in the solid phase, it is the measurement of the quantum yield associated with the solid (especially thin films) that would be the most meaningful, but it is the parameter that has been least reported relative to solution quantum yields. Even at that, the quantum yield values for amorphous solids, crystalline solids and thin films can vary. For the substituents shown in Figure 1.2, quantum yields in solution were generally reported but thin-film values were reported only for PyPySPyPy (28%) [41c], PPSPP ($\sim 62\%$) [41d], and the anthracenyl-substituted phenyl (which was 2.3 times the relative solid-state Φ_{PL} of DMPPS [41f]).

Several attempts have been made to molecularly engineer higher Φ_{PL} values and a few of the more recent reports are outlined here. Three publications concerning terminally substituted 2,5-alkynyl groups demonstrate how Φ_{PL} values of amorphous powders compare with the corresponding 2,3,4,5-tetraphenylsiloles although these were measured as thin films: $\text{Ph}_4\text{C}_4\text{SiMe}_2$ (73%), $\text{Ph}_4\text{C}_4\text{SiMePh}$ (95%), and $\text{Ph}_4\text{C}_4\text{SiPh}_2$ (94%) [24]. There were three series of 2,5-dialkynylsiloles and each series included the following substituents on silicon: Ph_2 , MePh , and Me_2 . Within each of the three series, the highest Φ_{PL} values (measured for amorphous solids) were found for the $\text{Ph}_2(\text{R}_3\text{SiC}\equiv\text{C})_2\text{C}_4\text{SiMePh}$ derivative [$\text{R} = \text{Me}$ (33.3%), Et (76.4%),

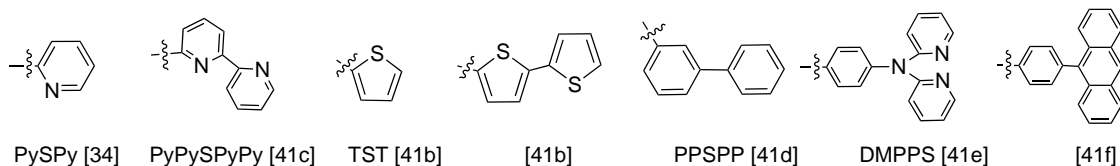


Figure 1.2 Selected examples of substituents incorporated at the 2,5-position using the Tamao procedure starting from $\text{Me}_2\text{Si}(\text{C}\equiv\text{CPh})_2$.

$i\text{Pr}$ (99.9%)). As the bulk of the R group in the silole increased the λ_{em} was blue shifted [42]. A later study of the same series as thin films but with $\text{Ph}_3\text{SiC}\equiv\text{C}-$ substituents gave lower Φ_{PL} values of 18.1% (SiPh_2), 28.3% (SiPhMe), and 34.6% (SiMe_2), the reverse of the order reported in the previous study by Tang's group [43]. An earlier study with a more complex 2,5-alkynyl substituent with phenyleneethynylene strands with up to three aromatic rings and a total of three alkynes also provided quantum yields for the solid state, but the values were less than 15% (the solid-state form was not specified) [44]. Another study included phenylacetylene dendrimers but these did not exhibit an AIE effect [45].

Other modifications with related sets of substituents have been described. In one study of various *p*-tolyl-substituted siloles, 1,1-dimethyl-2,5-bis(*p*-tolyl)-3,4-diphenylsilole, 1,1-dimethyl-2,5-diphenyl-3,4-bis(*p*-tolyl)silole, and 1,1-dimethyl-2,3,4,5-tetra(*p*-tolyl)silole were all prepared by the Tamao procedure for comparison with 1,1-dimethyl-2,3,4,5-tetraphenylsilole (DMTS). The maximum AIE enhancement was found for $\text{H}_2\text{O}-\text{THF}$ (95:5) and decreased in the order $\text{DMTS} > 3,4\text{-bis}(p\text{-tolyl}) > 2,3,4,5\text{-tetra}(p\text{-tolyl}) > 2,5\text{-bis}(p\text{-tolyl})$. The Me group is weakly electron donating and substitution results in a small bathochromic shift in absorbance maxima and a slight enhancement of luminescence quantum yields in the 2,5-substituted case versus the 3,4-substituted silole (consistent with the earlier summary by Marder and co-workers [5]) [46]. Another study involved the *core* structure of PyPySPyPy (see Figure 1.2) where the silicon center became part of a second ring (spirocycle) with five-membered (Cy5) and six-membered (Cy6) rings. The thin-film quantum yields for these spirocycles, compared with PyPySPyPy, which has two exocyclic methyl groups ($\Phi_{\text{PL}} = 28\%$), were only slightly higher for Cy5 (30%) and Cy6 (31%) [47a]. In a related study with 2,3,3',4,4'-hexaphenyl-1,1'-spirobisilole, the Φ_{PL} exhibited by the thin film was $55 \pm 5\%$, measured relative to Alq_3 (32%), although emission in solution was very weak ($\Phi_{\text{PL}} = 0.05\%$), consistent with the AIE effect [47b]. The Φ_{PL} values for solution (THF), aggregates (1:9 THF–water) and film have been reported to determine the effect of electron-accepting [$-\text{C}_6\text{H}_4\text{CH}=\text{C}(\text{CN})_2$] substituents versus electron-donating substituents [$-\text{C}_6\text{H}_4\text{N}(\text{Ph})_2$]. The values of $\Phi_{\text{PL}(\text{soln})}$, $\Phi_{\text{PL}(\text{aggr})}$, and $\Phi_{\text{PL}(\text{film})}$ were 0.2, 11.1, and 54.1%, respectively, for the electron-accepting group and 3.2, 44.1, and 74.0%, respectively, for the electron-donating group. These values show that not only is the form of the solid state important to use in comparisons but also electron-donating substituents provide higher Φ_{PL} values [48].

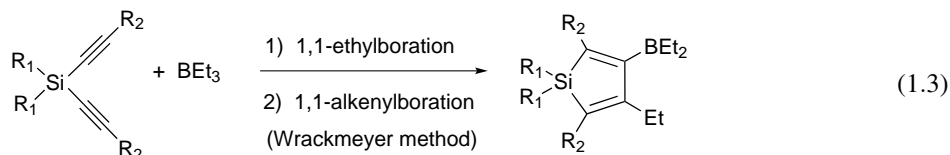
Under what conditions does a quenching reaction at the 2,5-positions in the Tamao procedure give unexpected products? An interesting case is the intended preparation of 2,5-bis(dimethylsilyl)-1,1-dimethyl-3,4-diphenylsilole. Quenching the dilithio intermediate with Me_2SiHCl gave not only the desired product in 48% yield but also an unexpected 3-silolene, 2,2,5,5-tetrakis(dimethylsilyl)-1,1-dimethyl-3,4-diphenyl-3-silolene (10%) resulting from further reduction. When the exocyclic substituents at silicon were either PhMe or Ph₂, the silolene did not form. The latter results were attributed to steric hindrance at silicon [49a]. In another case, also attributed to steric hindrance probably due to the four phenyl groups (two at the silicon center), the attempt to cross-couple the intermediate $\text{Ph}_2(\text{ClZn})_2\text{C}_4\text{SiPh}_2$ with a brominated tetraphenylethylene [catalyzed by $\text{Pd}(\text{PPh}_3)_2\text{Cl}_2$] resulted in homocoupling of the tetraphenylethylene to give 4,4'-bis(1,2,2-triphenylvinyl)biphenyl and no cross-coupling product [49b]. However, when a similar

reaction was conducted with one of the exocyclic phenyl substituents replaced by methyl, the targeted silole, 2,5-BTPEMTPS (prepared by the Tamao procedure, 35%) was isolated in 41% yield. 3,4-BTPEMTPS (35% yield) was also prepared using the Tamao procedure [49c]. The extent of the emission enhancement of the AIE effect can be related to the ratio of Φ_{aggr} to Φ_{soln} , that is, $\alpha_{\text{AIE}} = \Phi_{\text{aggr}}/\Phi_{\text{soln}}$. For 2,5-BTPEMTPS, $\Phi_{\text{soln}} = 0.34\%$ and $\Phi_{\text{film}} = 51.2\%$, whereas for 3,4-BTPEMTPS, $\Phi_{\text{soln}} = 0.38\%$ and $\Phi_{\text{film}} = 46.9\%$, giving an α_{AIE} of 150.6 for the 2,5-isomer and 123.4 for the 3,4-isomer. The corresponding α_{AIE} values for HPS and MePPS were 780 and 944. The differences between the two systems can be attributed to the presence of very bulky substituents for BTPEMTPS, which makes the phenyl rotors less free to undergo intramolecular rotations and therefore the Φ_{soln} values are higher than those of the ‘parent’ MPPS (or HPS). This consequently leads to a smaller value of α_{AIE} [49c]. However, the emission of the 2,5-isomer in both solution and aggregate states is more efficient than that of the 3,4-isomer, and the 2,5-isomer is electronically more conjugated (reflected in the greater red shift for the λ_{max} observed) than the 3,4-isomer [49c].

The Tamao procedure overcomes one of the inadequacies of the Curtis method in that it allows for the placement of substituents at the 2,5-positions that differ from those at the 3,4-positions (most often the 3,4-substituents are phenyl groups). This then allows for better electronic tuning, which has been shown to be most effective from the 2,5-positions. In addition, it is possible to incorporate selectively different substituents at each of these positions, thus allowing for incorporation of both electron-withdrawing and electron-donating substituents on the silole ring. The reactions at the 2,5-positions can be prone to steric hindrance to coupling, in which case reducing the bulk of the exocyclic substituents at silicon can alleviate this problem [49b,c]. An interesting, but not well-known, side aspect in the Tamao procedure is that copper-stabilized lithium cannot be used in the preparation of LiNaph as the reaction mixtures after addition of the LiNaph to the dialkynylsilane produce a gel and no silole product is observed. It is probable that the presence of copper promotes a different and unproductive reduction of the silole precursor, although this has not been verified. A limitation of the Tamao procedure is that the dialkynylsilane $\text{R}_2\text{Si}(\text{C}\equiv\text{C}\text{Ar})_2$ must have an aryl substituent that terminates the acetylene for a successful reductive coupling reaction. This restriction is removed in the Wrackmeyer approach, also involving dialkynylsilane precursors and which is described in the next section.

1.3.3 Intramolecular cyclization of dialkynylsilanes utilizing borane reagents

About a year before the Tamao reaction was introduced, the cyclization of $\text{R}_2\text{Si}(\text{C}\equiv\text{CR}')_2$ was introduced by Wrackmeyer and co-workers [50]. The overall reaction is shown in Equation 1.3 and has been proposed to occur in a two-step sequence involving 1,1-ethylboration followed by a 1,1-alkenylboration that provides the silole ring system. A unique feature of this ring closure method is that the terminal alkyne substituents are incorporated into the silole in the 2,5-positions. The early work on the 1,1-organoboration of alkynylsilicon compounds has been reviewed by Wrackmeyer [51].



In the majority of the publications on the generation of siloles by Wrackmeyer and co-workers, the products were characterized spectroscopically even when solvents were removed from the product mixtures to give oils. A variety of alkylboranes were used in the Wrackmeyer procedure, including R_3B with $\text{R} = \text{allyl}$